

# GeNIe: Generative Hard Negative Images Through Diffusion

Soroush Abbasi Koochpayegani<sup>\*,1</sup> Anuj Singh<sup>\*,2,3</sup>  
K L Navaneet<sup>1</sup> Hadi Jamali-Rad<sup>2,3</sup> Hamed Pirsiavash<sup>1</sup>

<sup>1</sup>University of California, Davis

<sup>2</sup>Delft University of Technology, The Netherlands

<sup>3</sup>Shell Global Solutions International B.V., Amsterdam, The Netherlands  
{soroush,nkadir,hpirsiav}@ucdavis.edu {a.r.singh,h.jamalirad}@tudelft.nl

**Abstract.** Data augmentation is crucial in training deep models, preventing them from overfitting to limited data. Recent advances in generative AI, e.g., diffusion models, have enabled more sophisticated augmentation techniques that produce data resembling natural images. We introduce **GeNIe** a novel augmentation method which leverages a latent diffusion model conditioned on a text prompt to merge contrasting data points (an image from the source category and a text prompt from the target category) to generate challenging samples. To achieve this, inspired by recent diffusion based image editing techniques, we limit the number of diffusion iterations to ensure the generated image retains low-level and background features from the source image while representing the target category, resulting in a hard negative sample for the source category. We further enhance the proposed approach by finding the appropriate noise level adaptively for each image (coined as **GeNIe-Ada**) leading to further performance improvement. Our extensive experiments, in both few-shot and long-tail distribution settings, demonstrate the effectiveness of our novel augmentation method and its superior performance over the prior art. Our code is available here: <https://github.com/UCDvision/GeNIe>

## 1 Introduction

Augmentation has become an integral part of training deep learning models, particularly when faced with limited training data. For instance, when it comes to image classification with limited number of samples per class, model generalization ability can be significantly hindered. Same goes with more complex tasks such as detection and segmentation in data-deficient settings. Simple transformations like rotation, cropping, and adjustments in brightness and contrast artificially diversify the training set, offering the model a more comprehensive grasp of potential data variations. Exposure to a broader range of augmented samples enhances model robustness, adaptability, and accuracy in predicting

---

\* equal contribution

novel instances. Hence, augmentation can serve as a practical strategy to boost model’s learning capacity, minimizing the risk of overfitting and facilitating effective knowledge transfer from limited labeled data to real-world scenarios.

Various image augmentation methods, encompassing standard transformations, and learning-based approaches have been proposed [15, 16]. Some augmentation approaches combine two images possibly from two different categories to generate a new sample image. The simplest ones in this category are MixUp [108] and CutMix [107] where two images are combined in the pixel space. However, the resulting image is usually not in the manifold of natural images, so it is unlikely for the model to see such images at test time.

Recently, leveraging generative models for data augmentation has gained an upsurge of attention. Inspired by diffusion-based image editing methods [77], we aim at using text-prompted latent diffusion models [78] for generating hard negative images. Our core idea (coined as **GeNIe**) is to sample source images from various categories and prompt the diffusion model with text corresponding to a different target category. We demonstrate that the choice of noise level (or equivalently number of iterations) for the diffusion process plays a pivotal role in generating images that semantically belong to the target category while retaining low-level features from the source image. We argue that these newly generated samples serve as *hard negatives* [61, 104] for the source category (or from a dual perspective hard positives for the target category). To further enhance **GeNIe**, we propose an adaptive noise level selection strategy (dubbed as **GeNIe-Ada**) enabling it to adjust the noise level automatically on a per-sample basis. **GeNIe** can aid addressing model performance challenges in the following scenarios.

**Data-deficient settings.** Real-world data often follows a long-tail distribution, where common scenarios dominate and rare occurrences (e.g., a person jaywalking a highway) are underrepresented. This lack of data poses challenges for training robust models, such as self-driving cars or surveillance systems. Same challenge arises in few-shot learning settings where model has to learn from only a handful of samples. **GeNIe** can generate meaningful augmentations to help boost model performance in both settings.

**Spurious correlations.** Visual features coincidentally present in certain categories can skew model decisions by inducing a bias towards co-occurrence of these features [29]. For instance, a giraffe on a highway is rare, causing models to struggle with such unusual scenarios. Combating this bias during model training is essential. A possible solution involves generating challenging examples that defy these biases. For example, by providing **GeNIe** with a street image and prompting it with “photo of a giraffe” one can generate out-of-distribution hard negatives for the street category.

Our extensive quantitative and qualitative experimentation, on a suite of few-shot and long-tail distribution settings corroborate the effectiveness of the proposed novel augmentation method (**GeNIe**, and its noise adaptive version, **GeNIe-Ada**), corroborating its significant impact on categories with a limited number of samples. A high-level sketch of **GeNIe** is illustrated in Figure 1. As can be seen, **GeNIe** can take as input a source image of a bunny and generate

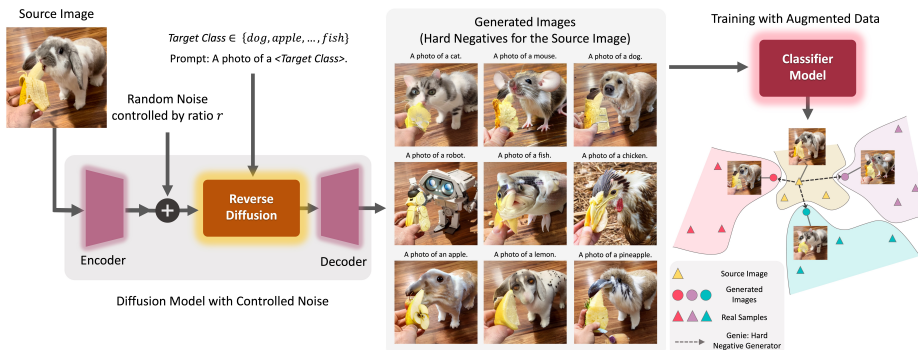


**Fig. 1: Generative Hard Negative Images Through Diffusion (GeNIe):** generates hard negative images that belong to the target category but are similar to the source image from low-level feature and contextual perspectives. To achieve this, GeNIe starts from a source image passing it through a partial noise addition process, and conditioning it on a different target category. By controlling the amount of noise, the reverse latent diffusion process generates images that can serve as hard negatives for the source category or hard positives for the target category.

images augmenting 9 different target categories in which the low-level features and background context of the source image are preserved.

## 2 Proposed Method: GeNIe

Given a source image  $X_S$  from category  $S = \langle \text{source category} \rangle$ , we are interested in generating a target image  $X_T$  from category  $T = \langle \text{target category} \rangle$ . In doing so, we intend to ensure the low-level visual features or background context of the source image are preserved, so that we generate samples that would serve as *hard negatives* for the *source* image. To this aim, we adopt a conditional latent diffusion model (such as Stable Diffusion, [78]) conditioned on a text prompt of the following format “A photo of a  $T = \langle \text{target category} \rangle$ ”.

**Key Idea.** GeNIe in its basic form is a simple yet effective augmentation sample generator for improving a classifier  $f_\theta(\cdot)$  with the following two key aspects: (i) inspired by [59, 63] instead of adding full amount of noise  $\sigma_{max}$  and going through all  $N_{max}$  (being typically 50) steps of denoising, we use less amount of noise ( $r\sigma_{max}$ , with  $r \in (0, 1)$ ) and consequently fewer number of denoising iterations ( $\lfloor rN_{max} \rfloor$ ); (ii) we prompt the diffusion model with a  $P$  mandating a target category  $T$  different than the source  $S$ . Hence, we denote the conditional diffusion process as  $X_T = \text{STDiff}(X_S, P, r)$ . In such a construct, the proximity of the final decoded image  $X_T$  to the source image  $X_S$  or the target category defined through the text prompt  $P$  depends on  $r$ . Hence, by controlling the amount of noise, we can generate images that blend characteristics of both the text prompt  $P$  and the source image  $X_S$ . If we do not provide much of visual details in the text prompt (e.g., desired background, etc.), we expect the decoded image  $X_T$  to follow the details of  $X_S$  while reflecting the semantics of the text

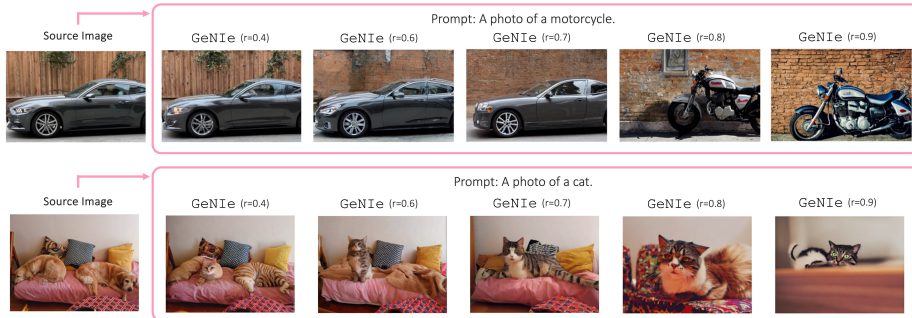


**Fig. 2: Effect of noise ratio,  $r$ , in GeNIe:** we employ GeNIe to generate augmentations for the target classes (motorcycle and cat) with varying  $r$ . Smaller  $r$  yields images closely resembling the source semantics, creating an inconsistency with the intended target label. By tracing  $r$  from 0 to 1, augmentations gradually transition from source image characteristics to the target category. However, a distinct shift from the source to the target occurs at a specific  $r$  that may vary for different source images or target categories. The generated images shift from car to motorcycle between  $r \in (0.7, 0.8)$  in the top row and from dog to cat at  $r \approx 0.4$  in the bottom row. For more examples, please see the supplementary material.

prompt  $P$ . We argue, and demonstrate later, that the newly generated samples can serve as *hard negative* examples for the source category  $S$  since they share the low-level features of  $X_S$  while representing the semantics of the target category,  $T$ . Notably, the source category  $S$  can be randomly sampled or be carefully extracted from the confusion matrix of  $f_\theta(\cdot)$  based on real training data. The latter might result in even *harder negative* samples being now cognizant of model confusions. Finally, we will append our initial dataset with the newly generated hard negative samples through GeNIe and (re)train the classifier model.

**Enhancing GeNIe: GeNIe-Ada.** One of the remarkable aspects of GeNIe lies in its simple application, requiring only  $X_S$ ,  $P$ , and  $r$ . However, selecting the appropriate value for  $r$  poses a challenge as it profoundly influences the outcome. When  $r$  is small, the resulting  $X_r$  tends to closely resemble  $X_S$ , and conversely, when  $r$  is large (closer to 1), it tends to resemble the semantics of the target category. This phenomenon arises because a smaller noise level restricts the capacity of the

diffusion model to deviate from the semantics of the input  $X_S$ . Thus, a critical question emerges: how can we select  $r$  for a particular source image to generate samples that preserve the low-level semantics of the source category  $S$  in  $X_S$  while effectively representing the semantics of the target category  $T$ ? We propose a method to determine an ideal value for  $r$ .

---

**Algorithm 1: GeNIe-Ada**

---

**Require:**  $X_S, X_T, f_\theta(\cdot), \text{STDiff}(\cdot), M$   
**1** Extract  $Z_S \leftarrow f_\theta(X_S), Z_T \leftarrow f_\theta(X_T)$   
**2** **for**  $m \in [1, M]$  **do**  
**3**      $r \leftarrow \frac{m}{M}, Z_r \leftarrow f_\theta(\text{STDiff}(X, P, r))$   
**4**      $d_m \leftarrow \frac{(Z_r - Z_S)^T (Z_T - Z_S)}{\|Z_r - Z_S\|_2}$   
**5** **end**  
**6**  $m^* \leftarrow \underset{m \in [2, M]}{\text{argmax}_m} |d_m - d_{m-1}|$   
**7**  $r^* \leftarrow \frac{m^*}{n}$   
**Return:**  $X_{r^*} = \text{STDiff}(X_S, P, r^*)$

---

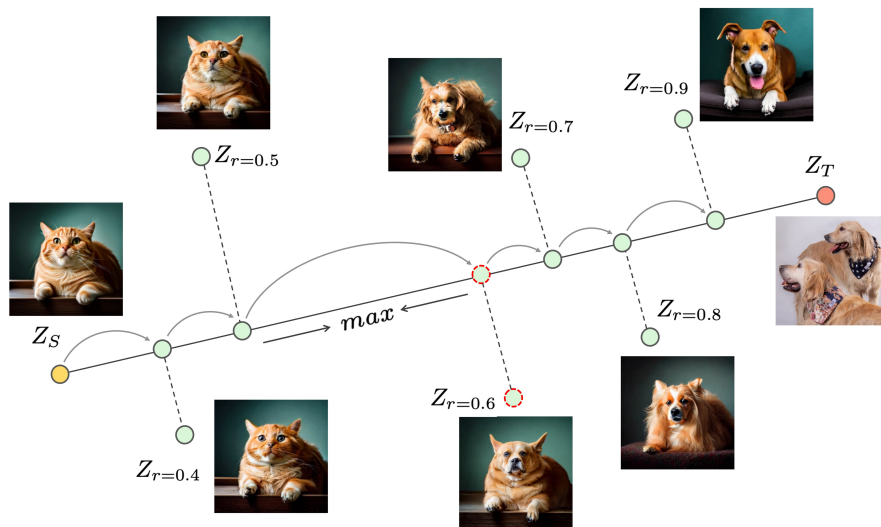


**Fig. 3: GeNIe-Ada:** To choose  $r$  adaptively for each (source image, target category) pair, we propose tracing the semantic trajectory from  $Z_S$  (source image embeddings) to  $Z_T$  (target embeddings) through the lens of the classifier  $f_\theta(\cdot)$  (Algorithm 1). We adaptively select the sample right after the largest semantic shift.

Our intuition suggests that by varying the noise ratio  $r$  from 0 to 1,  $X_r$  will progressively resemble category  $S$  in the beginning and category  $T$  towards the end. However, somewhere between 0 and 1,  $X_r$  will undergo a rapid transition from category  $S$  to  $T$ . This phenomenon is empirically observed in our experiments with varying  $r$ , as depicted in Figure 2. Even though the exact reason for this rapid change remains uncertain, one possible explanation is that the intermediate points between two categories reside far from the natural image manifold, thus, challenging the diffusion model’s capability to generate them. Ideally, we should select  $r$  corresponding to just after this rapid semantic transition, as at this point,  $X_r$  exhibits the highest similarity to the source image while belonging to the target category.

We propose to trace the semantic trajectory between  $X_S$  and  $X_T$  through the lens of the classifier  $f_\theta(\cdot)$ . As shown in Algorithm 1, assuming access to the classifier backbone  $f_\theta(\cdot)$  and at least one example  $X_T$  from the target category, we convert both  $X_S$  and  $X_T$  into their respective latent vectors  $Z_S$  and  $Z_T$  by passing them through  $f_\theta(\cdot)$ . Then, we sample  $M$  values for  $r$  uniformly distributed  $\in (0, 1)$ , generate their corresponding  $X_r$  and their latent vectors  $Z_r$  for all those  $r$ . Subsequently, we calculate  $d_r = \frac{(Z_r - Z_S)^T (Z_T - Z_S)}{\|Z_T - Z_S\|_2}$  as the distance between  $Z_r$  and  $Z_S$  projected onto the vector connecting  $Z_S$  and  $Z_T$ . Our hypothesis posits that the rapid semantic transition corresponds to a sharp change in this projected distance. Therefore, we sample  $n$  values for  $r$  uniformly distributed between 0 and 1, and analyze the variations in  $d_r$ . We identify the largest gap in  $d_r$  and select the  $r$  value just after the gap when increasing  $r$ . This is detailed in Algorithm 1 and illustrated in Figure 3.

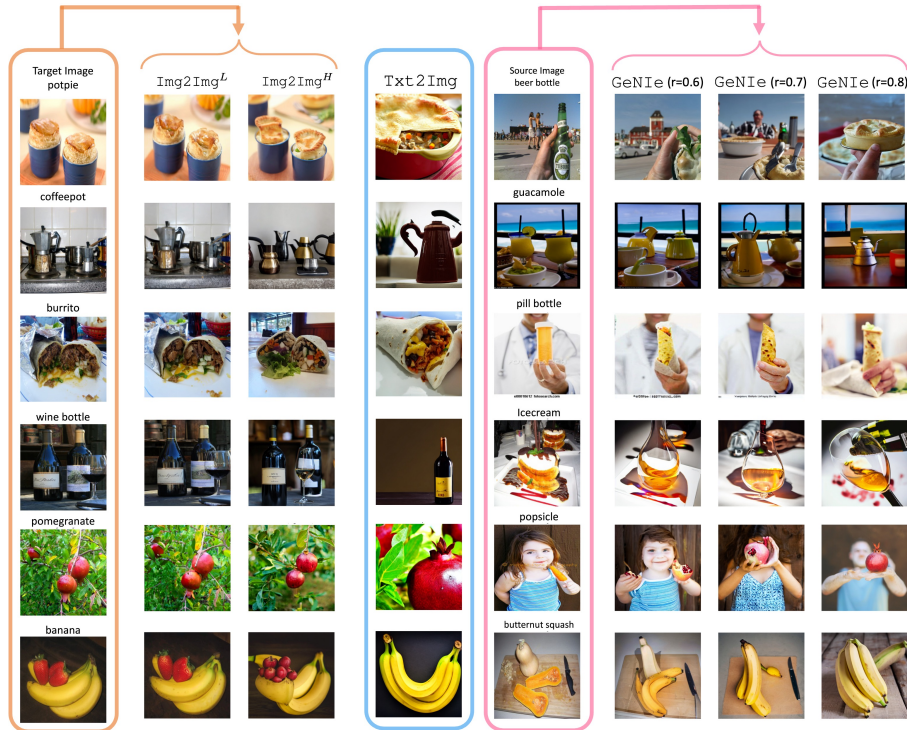


**Fig. 4: Visualization of Generative Samples:** We compare GeNIe with two baselines: **Img2Img<sup>L</sup> augmentation:** both image and text prompt are from the same category. Adding noise does not change the image much, so they are not hard examples. **Txt2Img augmentation:** We simply use the text prompt only to generate an image for the desired category (e.g., using a text2image method). Such images may be far from the domain of our task since the generation is not informed by any visual data from our task. **GeNIe augmentation:** We use target category name in the text prompt only along with the source image. We generate the desired images at appropriate amount of noise (80% in most cases). Note that we never define low-level features concretely and never evaluate if the augmented images preserves those features. That is our hypothesis only. We only evaluate if the augmented images help the accuracy.

### 3 Experiments

Since the impact of augmentation is more pronounced when the training data is limited, we evaluate the impact of GeNIe on Few-Shot classification in Sec 3.1, Long-Tailed classification in Sec 3.2, and fine-grained classification in Sec 3.3. For GeNIe-Ada in all scenarios, we utilize GeNIe to generate augmentations from the noise level set  $\{0.5, 0.6, 0.7, 0.8, 0.9\}$ . The selection of the appropriate noise level per source image and target is adaptive, achieved through Algorithm 1.

**Baselines.** We use Stable Diffusion 1.5 [78] as our base diffusion model. In all settings, we use the same prompt format to generate images for the target class: i.e., “A photo of a <target category>”, where we replace the **target category** with the target category label. We generate  $512 \times 512$  images for all methods.

For fairness in comparison, we generate the same number of new images for each class. We use a single NVIDIA RTX 3090 for image generation. We consider 2 diffusion-based baselines and a suite of traditional data augmentation baselines:

**Img2Img:** This baseline follows the data augmentation strategy based on Stable Diffusion proposed in [59, 63]. Concretely, we sample an image from a target class, add noise to its latent representation and then pass it along with a prompt for the target category through the reverse diffusion. Notice that the focus here is on a target class for which we generate extra positive samples. Adding large amount of noise (corresponding to large number of diffusion iterations) leads to generating an image less similar to the original image. We use two different noise magnitudes for this baseline:  $r = 0.3$  and  $r = 0.7$  and denote them by  $\text{Img2Img}^L$  and  $\text{Img2Img}^H$ , respectively.

**Txt2Img:** For this baseline, we omit the forward diffusion process and only use the reverse process starting from a text prompt for the target class of interest. This is similar to the base text-to-image generation strategy adopted in [4, 33, 58, 78, 84, 94]. Note that an extreme case of adding maximum noise ( $r = 0.999$ ) in  $\text{Img2Img}$  reduces it to  $\text{Txt2Img}$ .

**Traditional Data Augmentation:** We consider both weak and strong traditional augmentations. More specifically, for weak augmentation we use random resize crop with scaling  $\in [0.2, 1.0]$  and horizontal flipping. For strong augmentation, we consider random color jitter, random grayscale, and Gaussian blur. For the sake of completeness, we also compare against data augmentations such as CutMix [107] and MixUp [108] that combine two images together.

Figure 4 illustrate a set of generated augmentation examples for  $\text{Txt2Img}$ ,  $\text{Img2Img}$ , and **GeNIe**. As can be seen, **GeNIe** effectively generates hard negatives for the source image class by preserving its low-level features and transforming its main target class according to the prompt.

### 3.1 Few-shot Classification

We assess the impact of **GeNIe** compared to other forms of augmentation in a number of few-shot classification (FSL) scenarios, where the model has to learn only from the samples contained in the ( $N$ -way,  $K$ -shot) support set and infer on the query set. Note that this corresponds to an inference-only FSL setting where a pretraining stage on an abundant dataset is discarded. The goal is to assess how well the model can benefit from the augmented data samples while keeping the original  $N \times K$  samples intact.

**Datasets.** We conduct our few-shot experiments on two most commonly adopted few-shot classification datasets: *mini-Imagenet* [75] and *tiered-Imagenet* [76]. *mini-Imagenet* is a subset of ImageNet [20] for few-shot classification. It contains 100 classes with 600 samples each. We follow the predominantly adopted settings of [11, 75] where we split the entire dataset into 64 classes for training, 16 for validation and 20 for testing. *tiered-Imagenet* is a larger subset of ImageNet with 608 classes and a total of 779, 165 images, which are grouped into 34 higher-level nodes in the *ImageNet* human-curated hierarchy. This set of nodes

**Table 1: *mini-ImageNet*:** We use our augmentations on (5-way, 1-shot) and (5-way, 5-shot) few-shot settings of mini-Imagenet dataset with 3 different backbones (ResNet-18,34, and 50). We compare with various baselines and show that our augmentations with UniSiam method outperforms all the baselines including Txt2Img augmentation. The number of generated images per class is 4 for 1-shot and 20 for 5-shot settings.

ResNet-18					ResNet-34				
Augmentation	Method	Pre-training	1-shot	5-shot	Augmentation	Method	Pre-training	1-shot	5-shot
-	$\Delta$ -Encoder [82]	sup.	59.9	69.7	Weak	MatchingNet [96]	sup.	53.2±0.8	68.3±0.7
-	SNCA [101]	sup.	57.8±0.8	72.8±0.7	Weak	ProtoNet [88]	sup.	53.9±0.8	74.7±0.6
-	iDeMe-Net [14]	sup.	59.1±0.9	74.6±0.7	Weak	MAML [27]	sup.	51.5±0.9	65.9±0.8
-	Robust + dist [25]	sup.	63.7±0.6	81.2±0.4	Weak	RelationNet [90]	sup.	51.7±0.8	69.6±0.7
-	AFHN [50]	sup.	62.4±0.7	78.2±0.6	Weak	Baseline [11]	sup.	49.8±0.7	73.5±0.7
Weak	ProtoNet+SSL [89]	sup.+ssl	-	76.6	Weak	Baseline++ [11]	sup.	52.7±0.8	76.2±0.6
Weak	Neg-Cosine [53]	sup.	62.3±0.8	80.9±0.6	Weak	SimCLR [9]	unsup.	64.0±0.4	79.8±0.3
-	Centroid Align [1]	sup.	59.9±0.7	80.4±0.7	Weak	SimSiam [12]	unsup.	63.8±0.4	80.4±0.3
-	Baseline [11]	sup.	59.6±0.8	77.3±0.6	Weak	UniSiam+dist [57]	unsup.	<b>65.6±0.4</b>	<b>83.4±0.2</b>
-	Baseline++ [11]	sup.	59.0±0.8	76.7±0.6	Weak	UniSiam [57]	unsup.	64.3±0.8	82.3±0.5
Weak	PSST [13]	sup.+ssl	59.5±0.5	77.4±0.5	Strong	UniSiam [57]	unsup.	64.5±0.8	82.1±0.6
Weak	UMTRA [42]	unsup.	43.1±0.4	53.4±0.3	CutMix	UniSiam [57]	unsup.	64.0±0.8	81.7±0.6
Weak	ProtoCLR [62]	unsup.	50.9±0.4	71.6±0.3	MixUp	UniSiam [57]	unsup.	63.7±0.8	80.1±0.8
Weak	SimCLR [9]	unsup.	62.6±0.4	79.7±0.3	Img2Img <sup>L</sup>	UniSiam [57]	unsup.	65.5±0.8	82.9±0.5
Weak	SimSiam [12]	unsup.	62.8±0.4	79.9±0.3	Img2Img <sup>H</sup>	UniSiam [57]	unsup.	70.5±0.8	84.8±0.5
Weak	UniSiam+dist [57]	unsup.	<b>64.1±0.4</b>	<b>82.3±0.3</b>	Txt2Img	UniSiam [57]	unsup.	75.4±0.6	85.5±0.5
Weak	UniSiam [57]	unsup.	63.1±0.8	81.4±0.5	GeNIe (Ours)	UniSiam [57]	unsup.	<b>77.1±0.6</b>	<b>86.3±0.4</b>
Strong	UniSiam [57]	unsup.	62.8±0.8	81.2±0.6	GeNIe-Ada (Ours)	UniSiam [57]	unsup.	<b>78.5±0.6</b>	<b>86.6±0.4</b>
CutMix	UniSiam [57]	unsup.	62.7±0.8	80.6±0.6	<b>ResNet-50</b>				
MixUp	UniSiam [57]	unsup.	62.1±0.8	80.7±0.6	Weak	UniSiam [57]	unsup.	64.6±0.8	83.4±0.5
Img2Img <sup>L</sup>	UniSiam [57]	unsup.	63.9±0.8	82.1±0.5	Strong	UniSiam [57]	unsup.	64.8±0.8	83.2±0.5
Img2Img <sup>H</sup>	UniSiam [57]	unsup.	69.1±0.7	84.0±0.5	CutMix	UniSiam [57]	unsup.	64.3±0.8	83.2±0.5
Txt2Img	UniSiam [57]	unsup.	74.1±0.6	84.6±0.5	MixUp	UniSiam [57]	unsup.	63.8±0.8	84.6±0.5
GeNIe (Ours)	UniSiam [57]	unsup.	<b>75.5±0.6</b>	<b>85.4±0.4</b>	Img2Img <sup>L</sup>	UniSiam [57]	unsup.	66.0±0.8	84.0±0.5
GeNIe-Ada (Ours)	UniSiam [57]	unsup.	<b>76.8±0.6</b>	<b>85.9±0.4</b>	Img2Img <sup>H</sup>	UniSiam [57]	unsup.	71.1±0.7	85.7±0.5
					Txt2Img	UniSiam [57]	unsup.	76.4±0.6	86.5±0.4
					GeNIe (Ours)	UniSiam [57]	unsup.	<b>77.3±0.6</b>	<b>87.2±0.4</b>
					GeNIe-Ada (Ours)	UniSiam [57]	unsup.	<b>78.6±0.6</b>	<b>87.9±0.4</b>

is partitioned into 20, 6, and 8 disjoint sets of training, validation, and testing nodes, and the corresponding classes form the respective meta-sets.

**Evaluation.** To quantify the impact of different augmentation methods, we evaluate the test-set accuracies of a state-of-the-art unsupervised few-shot learning method with GeNIe and compare them against the accuracies obtained using other augmentation methods. Specifically, we use UniSiam [57] pre-trained with ResNet-18, ResNet-34 and ResNet-50 backbones and follow its evaluation strategy of fine-tuning a logistic regressor to perform ( $N$ -way,  $K$ -shot) classification on the test sets of *mini*- and *tiered*-Imagenet. Following [75], an episode consists of a labeled support-set and an unlabelled query-set. The support-set contains  $N$  randomly sampled classes where each class contains  $K$  samples, whereas the query-set contains  $Q$  randomly sampled unlabeled images per class. We conduct our experiments on the two most commonly adopted settings: (5-way, 1-shot) and (5-way, 5-shot) classification settings. Following the literature, we sample 16-shots per class for the query set in both settings. We report the test accuracies along with the 95% confidence interval over 600 and 1000 episodes for *mini*-ImageNet and *tiered*-ImageNet, respectively.

**Implementation Details:** GeNIe generates augmented images for each class using images from all other classes as the source image. Specifically, we generate 4 samples per class as augmentations in the 5-way, 1-shot setting and 20 samples per class as augmentations in the 5-way, 5-shot setting. For the sake of a fair comparison, we ensure that the total number of labeled samples in the



support set after augmentation remains the same across all different traditional and generative augmentation methodologies.

**Results:** The results on *mini*-Imagenet and *tiered*-Imagenet for both (5-way, 1 and 5-shot) settings are summarized in Table 1 and Table 2, respectively. Regardless of the choice of backbone, we observe that GeNIe helps consistently improve UniSiam’s performance and outperform other supervised and unsupervised few-shot classification methods as well as other data augmentation techniques on both datasets, across both (5-way, 1 and 5-shot) settings. Our noise adaptive method of selecting optimal augmentations per source image (GeNIe-Ada) further improves GeNIe’s performance across all three backbones, both few-shot settings, and both datasets (*mini* and *tiered*-Imagenet). We note that employing CutMix and MixUp diminishes performance compared to weak augmentations. We hypothesize this is due to overfitting of CutMix and MixUp since they can choose from only 4 other classes to mix.

### 3.2 Long-Tailed Classification

We evaluate our method in Long-Tailed data, where number of instances per class is not balanced and most categories have limited samples (tail). Our goal is to mitigate this bias by augmenting the tail of the distribution with generated samples. Following LViT [103], first, we train an MAE [31] on the unbalanced dataset without any augmentation. We then train the Balanced Fine Tuning stage of LViT by incorporating the augmentation data generated using GeNIe or the other baselines.

**Dataset:** We perform experiments on ImageNet-LT [56]. It contains 115.8K images from 1,000 categories. The number of images per class vary from 1280 to 5. Imagenet-LT classes can be divided into 3 groups: “Few” with less than 20 images, “Med” with 20 – 100 images, and “Many” with more than 100 images. Imagenet-LT uses the same validation set as ImageNet. We generate new data for the “Few” categories only. We limit the number of generated images to 50 samples per class. For GeNIe, instead of randomly sampling the source images from other classes, we use confusion matrix on the training data to find top-4 most confused classes and only consider those classes for random sampling of the source image. The source category may be from “Many”, “Med”, or “Few sets”.

**Implementation Details:** We download the pretrained ViT-B of LViT [103] and finetune it with Bal-BCE loss proposed therein on the augmented dataset. Training takes 2 hours on four NVIDIA RTX 3090 GPUs. We use the same hyperparameters as in [103] for finetuning: 100 epochs,  $lr = 0.008$ , batch size of 1024, CutMix and MixUp for the data augmentation.

**Results:** The results are summarized in Table 3. Augmenting training data with GeNIe-Ada improves accuracy on the “Few” set by 11.7% and 4.4% compared with LViT only and LViT with Txt2Img augmentation baselines respectively. Moreover, GeNIe-Ada improves the overall accuracy by 2.2% compared to the baselines with only traditional augmentations.

**Table 2: *tiered-ImageNet*:** Accuracies (%  $\pm$  std) for 5-way, 1-shot and 5-way, 5-shot classification settings on the test-set. We compare against various SOTA supervised and unsupervised few-shot classification baselines as well as other augmentation methods, with UniSiam [57] pre-trained ResNet-18, 34 and 50 backbones. UniSiam+dist indicates that the backbone was pre-trained with a ResNet-50 teacher.

ResNet-18				
Augmentation	Method	Pre-training	1-shot	5-shot
-	Transd-CNAPS [5]	sup.	65.9 $\pm$ 1.0	81.8 $\pm$ 0.7
-	FEAT [105]	sup.	70.8	84.8
Weak	SimCLR [9]	unsup.	63.4 $\pm$ 0.4	79.2 $\pm$ 0.3
Weak	SimSiam [12]	unsup.	64.1 $\pm$ 0.4	81.4 $\pm$ 0.3
Weak	UniSiam + dist [57]	unsup.	67.0 $\pm$ 0.4	84.5 $\pm$ 0.3
Weak	UniSiam [57]	unsup.	63.1 $\pm$ 0.7	81.0 $\pm$ 0.5
Strong	UniSiam [57]	unsup.	62.8 $\pm$ 0.7	80.9 $\pm$ 0.5
CutMix	UniSiam [57]	unsup.	62.1 $\pm$ 0.7	78.9 $\pm$ 0.6
MixUp	UniSiam [57]	unsup.	62.1 $\pm$ 0.7	78.4 $\pm$ 0.6
Img2Img <sup>L</sup>	UniSiam [57]	unsup.	63.9 $\pm$ 0.7	81.8 $\pm$ 0.5
Img2Img <sup>H</sup>	UniSiam [57]	unsup.	68.7 $\pm$ 0.7	83.5 $\pm$ 0.5
Trt2Img	UniSiam [57]	unsup.	72.9 $\pm$ 0.6	84.2 $\pm$ 0.5
GeNIe (Ours)	UniSiam [57]	unsup.	<b>73.6<math>\pm</math>0.6</b>	<b>85.0<math>\pm</math>0.4</b>
GeNIe-Ada (Ours)	UniSiam [57]	unsup.	<b>75.1<math>\pm</math>0.6</b>	<b>85.5<math>\pm</math>0.5</b>
ResNet-34				
Weak	UniSiam + dist [57]	unsup.	68.7 $\pm$ 0.4	85.7 $\pm$ 0.3
Weak	UniSiam [57]	unsup.	65.0 $\pm$ 0.7	82.5 $\pm$ 0.5
Strong	UniSiam [57]	unsup.	64.8 $\pm$ 0.7	82.4 $\pm$ 0.5
CutMix	UniSiam [57]	unsup.	63.8 $\pm$ 0.7	80.3 $\pm$ 0.6
MixUp	UniSiam [57]	unsup.	64.1 $\pm$ 0.7	80.0 $\pm$ 0.6
Img2Img <sup>L</sup>	UniSiam [57]	unsup.	66.1 $\pm$ 0.7	83.1 $\pm$ 0.5
Img2Img <sup>H</sup>	UniSiam [57]	unsup.	70.4 $\pm$ 0.7	84.7 $\pm$ 0.5
Trt2Img	UniSiam [57]	unsup.	75.0 $\pm$ 0.6	85.4 $\pm$ 0.4
GeNIe (Ours)	UniSiam [57]	unsup.	<b>75.7<math>\pm</math>0.6</b>	<b>86.0<math>\pm</math>0.4</b>
GeNIe-Ada (Ours)	UniSiam [57]	unsup.	<b>76.9<math>\pm</math>0.6</b>	<b>86.3<math>\pm</math>0.2</b>
ResNet-50				
Weak	UniSiam + dist [57]	unsup.	69.6 $\pm$ 0.4	86.5 $\pm$ 0.3
Weak	UniSiam [57]	unsup.	66.8 $\pm$ 0.7	84.7 $\pm$ 0.5
Strong	UniSiam [57]	unsup.	66.5 $\pm$ 0.7	84.5 $\pm$ 0.5
CutMix	UniSiam [57]	unsup.	66.0 $\pm$ 0.7	83.3 $\pm$ 0.5
MixUp	UniSiam [57]	unsup.	66.1 $\pm$ 0.5	84.1 $\pm$ 0.8
Img2Img <sup>L</sup>	UniSiam [57]	unsup.	67.8 $\pm$ 0.7	85.3 $\pm$ 0.5
Img2Img <sup>H</sup>	UniSiam [57]	unsup.	72.4 $\pm$ 0.7	86.7 $\pm$ 0.4
Trt2Img	UniSiam [57]	unsup.	77.1 $\pm$ 0.6	87.3 $\pm$ 0.4
GeNIe (Ours)	UniSiam [57]	unsup.	<b>78.0<math>\pm</math>0.6</b>	<b>88.0<math>\pm</math>0.4</b>
GeNIe-Ada (Ours)	UniSiam [57]	unsup.	<b>78.8<math>\pm</math>0.6</b>	<b>88.6<math>\pm</math>0.6</b>

### 3.3 Fine-grained Few-shot Classification

To further investigate the impact of the proposed method, we compare GeNIe with other text-based data augmentation techniques across four distinct fine-grained datasets in a 20-way, 1-shot classification setting. We employ the pre-trained DinoV2 ViT-G [66] backbone as a feature extractor to derive features from training images. Subsequently, an SVM classifier is trained on these features, and we report the Top-1 accuracy of the model on the test set.

**Datasets:** We assess our method on several datasets: Food101 [6] with 101 classes of various foods, CUB200 [97] with 200 bird species classes, Cars196 [45] with 196 car model classes, and FGVC-Aircraft [60] with 41 aircraft manufacturer classes. Further details on each dataset can be found in Section A.2. The reported metric is the average Top-1 accuracy over 100 episodes. Each episode involves sampling 20 classes and 1-shot from the training set, with the final model evaluated on the respective test set.

**Table 3: Long-Tailed ImageNet-LT:** We compare different augmentation methods on ImageNet-LT and report Top-1 accuracy for “Few”, “Medium”, and “Many” sets. On the “Few” set and LiVT method, our augmentations improve the accuracy by 11.7 points compared to LiVT original augmentation and 4.4 points compared to Txt2Img. Refer to Table A1 for a full comparison with prior Long-Tailed methods.

ViT-B					
Method	Resolution	Many	Med.	Few	Overall Acc
LiVT [103]	384	76.4	59.7	42.7	63.8
ViT [22]	224	50.5	23.5	6.9	31.6
MAE [30]	224	74.7	48.2	19.4	54.5
DeiT [93]	224	70.4	40.9	12.8	48.4
LiVT [103]	224	73.6	56.4	41.0	60.9
LiVT + Img2Img <sup>L</sup>	224	74.3	56.4	34.3	60.5
LiVT + Img2Img <sup>H</sup>	224	73.8	56.4	45.3	61.6
LiVT + Txt2Img	224	<b>74.9</b>	55.6	48.3	62.2
LiVT + GeNIe (r=0.8)	224	74.5	56.7	50.9	62.8
LiVT + GeNIe-Ada	224	74.0	<b>56.9</b>	<b>52.7</b>	<b>63.1</b>

**Table 4: Few-shot Learning on Fine-grained dataset:** We utilize a SVM classifier trained atop the DinoV2 ViT-G pre-trained backbone, reporting Top-1 accuracy for the test set of each dataset. The baseline is an SVM trained on the same backbone using weak augmentation. Across all datasets, GeNIe surpasses this baseline.

Method	CUB200 [97]	Cars196 [45]	Food101 [6]	Aircraft [60]
Baseline	90.3	49.8	82.9	29.2
Img2Img <sup>L</sup>	90.7	50.4	87.4	31.0
Img2Img <sup>H</sup>	91.3	56.4	91.7	34.7
Txt2Img	92.0	81.3	93.0	41.7
GeNIe (r=0.5)	92.0	84.6	91.5	39.8
GeNIe (r=0.6)	92.2	87.1	92.5	45.0
GeNIe (r=0.7)	92.5	<b>87.9</b>	92.9	<b>47.0</b>
GeNIe (r=0.8)	92.5	87.7	<b>93.1</b>	46.5
GeNIe (r=0.9)	92.4	87.1	<b>93.1</b>	45.7
GeNIe-Ada	<b>92.6</b>	<b>87.9</b>	<b>93.1</b>	46.9

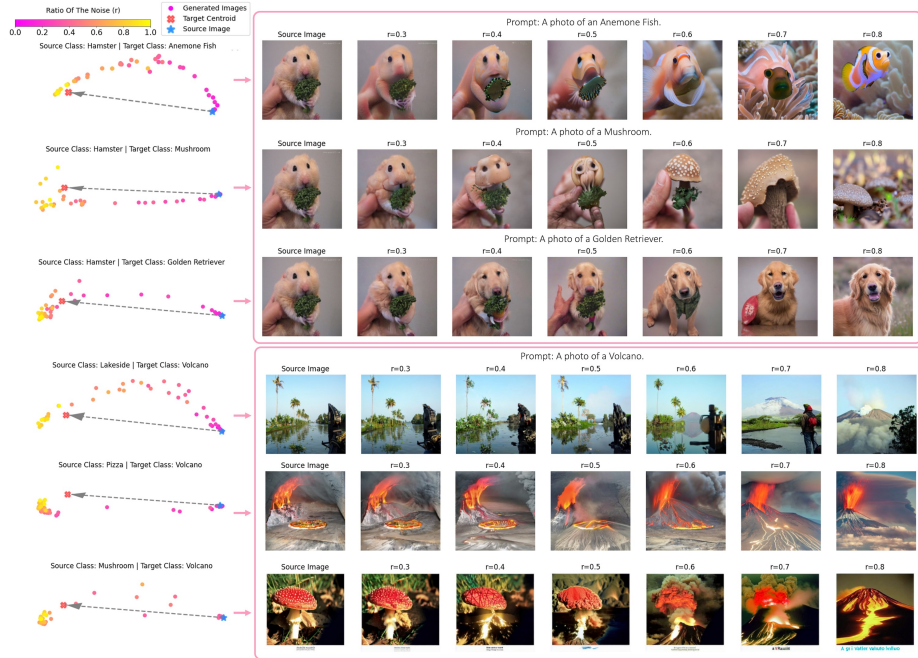


**Fig. 5: Embedding visualizations of generative augmentations:** We pass all generative augmentations through DinoV2 ViT-G (serving as an oracle) to extract their corresponding embeddings and visualize them with PCA. As depicted above, the extent of semantic shifts varies based on both the source image and the target class.

**Implementation Details:** We enhance the basic prompt by incorporating the superclass name for the fine-grained dataset: “A photo of a `<target class>`, a type of `<superclass>`”. For instance, in the *food* dataset and the *burger* class, our prompt reads: “A photo of a *burger*, a type of *food*.” No additional augmentation is used for generative methods in this context. We generate 19 samples for both cases of our method and also the baseline with weak augmentation.

**Results:** Table 4 summarizes the results. GeNIe helps outperform all other baselines and augmentations, including Txt2Img, by margins upto 0.5% on CUB200 [97], 6.6% on Cars196 [45], 0.1% on Food101 [6] and 5.3% on FGVC-Aircraft [60]. Notably, GeNIe exhibits great effectiveness in more challenging datasets, outperforming the baseline with traditional augmentation by about 38% for the Cars dataset and by roughly 17% for the Aircraft dataset. It can be observed here that GeNIe-Ada performs on-par with GeNIe with fix noise level, eliminating the necessity for noise level search in GeNIe.

### 3.4 Ablation and Analysis

**Semantic shift from source to target class.** The core motivation behind GeNIe-Ada is that by varying the noise ratio  $r$  from 0 to 1,  $X_r$  will progressively shift its semantic category from  $S$  in the beginning to category  $T$  towards the

**Table 5: Effect of Noise in GeNIe:** We use the same setting as in Table 1 to study the effect of the amount of noise. As expected (also shown in Fig 5), small noise results in worse accuracy since some generated images may be from the source category rather than the target one. For  $r = 0.5$  only 73% of the generated data is from the target category. This behavior is also shown in Figure 2. Notably, reducing the noise level below 0.7 is associated with a decline in oracle accuracy and a subsequent degradation in the performance of the final few-shot model. Note that high oracle accuracy of GeNIe-Ada demonstrates its capability to adaptively select the noise level per source and target, ensuring semantic consistency with the intended target.

Noise	ResNet-18		ResNet-34		ResNet-50		Oracle Acc
	1-shot	5-shot	1-shot	5-shot	1-shot	5-shot	
GeNIe( $r=0.5$ )	60.42±0.8	74.11±0.6	62.02±0.8	75.80±0.6	63.65±0.9	77.61±0.6	73.4±0.5
GeNIe( $r=0.6$ )	69.66±0.7	80.65±0.5	71.13±0.7	82.21±0.5	72.10±0.7	82.79±0.5	85.8±0.4
GeNIe( $r=0.7$ )	74.50±0.6	83.26±0.5	76.41±0.6	84.44±0.5	77.05±0.6	84.95±0.4	94.5±0.2
GeNIe( $r=0.8$ )	75.45±0.6	85.38±0.4	77.08±0.6	86.28±0.4	77.28±0.6	87.22±0.4	98.2±0.1
GeNIe( $r=0.9$ )	74.96±0.6	85.29±0.4	77.63±0.6	86.17±0.4	77.73±0.6	87.00±0.4	99.3±0.1
GeNIe-Ada	76.79±0.6	85.89±0.4	78.49±0.6	86.55±0.4	78.64±0.6	87.88±0.4	98.9±0.2

end. However, somewhere between 0 and 1,  $X_r$  will undergo a rapid transition from  $S$  to  $T$ . To demonstrate this hypothesis empirically, in Figure 5 and A3, we visualize two pairs of source images and target categories with their respective GeNIe generated augmentations for different noise ratios  $r$ , along with their corresponding PCA-projected embedding scatter plots. Note that we extract embeddings for all the images using a DinoV2 ViT-G pretrained backbone, which we assume as an oracle in identifying the category. We observe that as  $r$  increases from 0.3 to 0.8, the images transition to embody more of the target category’s semantics while preserving the contextual features of the source image. This transition of semantics can also be observed in the embedding plot where the embeddings consistently shift from the proximity of the source image to the target class’s centroid as the noise ratio  $r$  increases. Note that since embeddings for larger  $r$  are closer to the target category, we call them *hard negatives* for source category or *hard positives* for target category. Moreover, the sparse distribution of points at  $r = [0.5, 0.6]$  for the second image and  $r = [0.3, 0.4]$  for the third image corroborates with our intuition of a rapid transition from category  $S$  to  $T$ , thus empirically affirming our motivation behind GeNIe-Ada.

**Label consistency of the generated samples.** As mentioned earlier, the choice of noise ratio  $r$  is important in producing hard negative examples. In Table 5, we present the accuracy of the GeNIe model across various noise ratios, alongside the oracle accuracy, which is an ImageNet-pretrained DeiT-Base [92] classifier. We observe a decline in the label consistency of generated data (quantified by the performance of the oracle model) when decreasing the noise level. Reducing  $r$  also results in a degradation in the performance of the final few-shot model (87.2%  $\rightarrow$  77.6%) corroborating that an appropriate choice of  $r$  plays a crucial role in our design strategy. We investigate this further in the following paragraph.

**Effect of Noise in GeNIe.** We examine the impact of noise on the performance of the few-shot model, summarizing the findings in Table 5. Our observations

indicate that noise levels  $r \in [0.7, 0.8]$  yield the best performance. Conversely, utilizing noise levels below 0.7 diminishes performance due to label inconsistency, as is demonstrated in Table 5 and Fig 5. As such, determining the appropriate noise level is pivotal for the performance of GeNIe to be able to generate challenging hard negatives while maintaining label consistency. An alternative approach to finding the optimal noise level involves using GeNIe-Ada to adaptively select the noise level for each source image and target class. As demonstrated in Tables 5 and 4, GeNIe-Ada achieves performance that is comparable to or surpasses that of GeNIe with fixed noise levels.

**Limitation.** We assess the augmentation time for each image on a single RTX 3090 GPU, which varies with different noise levels requiring varying reverse diffusion iterations. For 512 by 512 resolution images, augmenting takes 4.4 seconds at  $r = 0.5$  and 6.7 seconds at  $r = 0.8$ . Notably, this is slower than traditional methods like cropping and resizing, limiting GeNIe to online image augmentation. However, this constraint could be mitigated through advancements in diffusion model efficiency. Recent diffusion models [54, 64, 81] notably enhance runtime. Evaluating these models is out of the scope for this paper.

Furthermore, we anticipate that GeNIe may encounter challenges when applied to datasets where the images deviate from the distribution expected by the generative backbone or when category names are unfamiliar to the text encoder within the generative method. It’s important to note that this limitation extends to any augmentation methods rooted in text-to-image generative approaches. A potential resolution lies in fine-tuning the text-to-image generative model on a small set of image-text pairs relevant to the downstream task. By doing so, the generative model becomes more attuned to the unique characteristics of the task, enhancing its effectiveness when employed as a data augmentation technique.

## 4 Related Work

**Data Augmentations:** Data augmentation is a simple, yet effective way to improve generalization of deep learning models. Recent contrastive self-supervised learning methods also heavily depend on data augmentation [10, 32, 44]. Simple flipping, cropping, color jittering, and blurring are some forms of weak and strong augmentations. The strength of augmentation is the extent of image distortion following the application of each augmentation [86]. However, using data augmentation is not trivial on some domains (e.g., medical). For example, using blurring might remove important low level information from images. More advanced approaches, such as MixUp [108] and CutMix [107], mix images and their labels accordingly [17, 35, 43, 55], which seem to offer better model generalization and robustness as well. However, the augmented (mixed) images are now not natural anymore and thus training proceeds on out of distribution images. Another strand of research tailors the augmentation strategy to fit the data, as seen in studies such as [15, 16, 21]. Unlike the above methods, we propose to utilize pretrained diffusion models to augment the training data. Note that generative models are indeed trained to generate natural images; however, the typical challenge here is that the generated images might not necessarily belong to same

data distribution as the training dataset, which could entail further finetuning them to the specific domain.

**Data Augmentation with Generative Models:** Generative models could be used to generate images within the manifold of natural images. Using synthesized images from generative models to augment training data have been studied before in many domains [28, 80], including domain adaptation [38], visual alignment [67], and mitigation of dataset bias [34, 83]. [69] introduce a methodology aimed at enhancing test set evaluation through augmentation. While previous methods predominantly relied on GANs [48, 95, 111] as the generative model, more recent studies promote using diffusion models [78] to augment the data. More specifically, [4, 33, 58, 84, 94] study the effectiveness of text-to-image diffusion models in data augmentation by diversification of each class with synthetic images. [39] uses an SVM in the latent space of the CLIP model to find spurious correlations and generates challenging examples using a diffusion model. [26] use CLIP model to filter generated images. Along the same lines, [24] utilize text-based diffusion and a language model to diversify the training data. From this angle, Boomerang [59] and SDEdit [63] are the closest approaches to our method. They they edit each data samples (source images) by adding small amount of noise to each image and applying reverse diffusion to generate an augmented image close to the source image. Unlike Boomerang, we set the negatives classes as source and employ the generative model to transform it to have the semantics of the positive class (Target class) while preserving the visual futures of the negative samples, which is the key reason why we argue these newly generated samples are now *hard negatives* [61, 104]. In a nutshell, the aforementioned studies focus on improving diversity of each class with effective prompts and diffusion models, however, we focus on generating effective hard negative samples for each class by combining two sources of contradicting information (images from the source category and text prompt from the target category.)

**Language Guided Recognition Models:** Language-vision foundation models have recently received an upsurge of attention [2, 72–74, 78, 79]. These models use human language to guide generating images, or extracting features from images which are aligned with human languages. Due to alignment with human language, these models can be used in downstream recognition tasks. For example, CLIP [72] shows decent zero-shot performance on many downstream tasks by matching image to their text descriptions. Some recent works improve utilization of human language in the prompt [23, 68], and others use a diffusion model directly as classifier [46]. Similar to the above, we use a foundation model (Stable Diffusion 1.5 [78]) to improve the downstream task. Concretely, we utilize category names of the downstream tasks to augment their associate training data with hard negative samples.

**Few-Shot Learning:** revolves around learning very fast from only a handful of samples. FSL is typically conducted in two stages: pretraining on an abundance of data followed by fast adaptation to unseen few-shot episodes. Each episode consists of a support set allowing the model to adapt itself quickly to the unseen classes, and a query set on which the model is evaluated. In supervised

FSL [1, 11, 25, 50, 70, 87, 90, 106, 113], pretraining is done on a labeled dataset, whereas in unsupervised FSL [3, 37, 40, 42, 57, 62, 71, 85, 98] the pretraining has to be conducted on an unlabeled dataset posing an extra challenge in the learning paradigm and neighboring these methods closer to the realm of self-supervised learning. Even though FSL is not of primal interest in this work, we assess the impact of GeNIe on a number of few-shot scenarios and state-of-the-art baselines by accentuating on its impact on the few-shot inference stage.

## 5 Conclusion

GeNIe leverages diffusion models to generate challenging samples for the target category while retaining some low-level and contextual features from the source image. Our experiments, spanning few-shot and long-tail distribution settings, showcase GeNIe’s effectiveness, especially in categories with limited examples. We hope our paper facilitates developing better hard-negative augmentation methods with the advancement of generative AI methods.

**Acknowledgments.** This work is partially funded by NSF grant number 1845216, DARPA Contract No. HR00112290115, and Shell.ai Innovation Program at Shell Global Solutions International B.V.

## References

1. Afrasiyabi, A., Lalonde, J.F., Gagné, C.: Associative alignment for few-shot image classification. In: ECCV (2019)
2. Alayrac, J.B., Donahue, J., Luc, P., Miech, A., Barr, I., Hasson, Y., Lenc, K., Mensch, A., Millican, K., Reynolds, M., Ring, R., Rutherford, E., Cabi, S., Han, T., Gong, Z., Samangooei, S., Monteiro, M., Menick, J., Borgeaud, S., Brock, A., Nematzadeh, A., Sharifzadeh, S., Binkowski, M., Barreira, R., Vinyals, O., Zisserman, A., Simonyan, K.: Flamingo: a visual language model for few-shot learning (2022)
3. Antoniou, A., Storkey, A.: Assume, augment and learn: Unsupervised few-shot meta-learning via random labels and data augmentation. arxiv:1902.09884 (2019)
4. Azizi, S., Kornblith, S., Saharia, C., Norouzi, M., Fleet, D.J.: Synthetic data from diffusion models improves imagenet classification (2023)
5. Bateni, P., Barber, J., van de Meent, J.W., Wood, F.: Enhancing few-shot image classification with unlabelled examples. In: Proceedings of the IEEE/CVF Winter Conference on Applications of Computer Vision (WACV). pp. 2796–2805 (January 2022)
6. Bossard, L., Guillaumin, M., Van Gool, L.: Food-101 – mining discriminative components with random forests. In: European Conference on Computer Vision (2014)
7. Cai, J., Wang, Y., Hwang, J.N., et al.: Ace: Ally complementary experts for solving long-tailed recognition in one-shot. In: ICCV. pp. 112–121 (2021)
8. Cao, K., Wei, C., Gaidon, A., Arechiga, N., Ma, T.: Learning imbalanced datasets with label-distribution-aware margin loss. NeurIPS **32** (2019)

9. Chen, T., Kornblith, S., Norouzi, M., Hinton, G.: A simple framework for contrastive learning of visual representations. In: ICML (2020)
10. Chen, T., Kornblith, S., Norouzi, M., Hinton, G.: A simple framework for contrastive learning of visual representations. In: ICML. pp. 1597–1607. PMLR (2020)
11. Chen, W.Y., Liu, Y.C., Kira, Z., Wang, Y.C.F., Huang, J.B.: A closer look at few-shot classification. In: ICLR (2019)
12. Chen, X., He, K.: Exploring simple siamese representation learning. In: CVPR (2021)
13. Chen, Z., Ge, J., Zhan, H., Huang, S., Wang, D.: Pareto self-supervised training for few-shot learning. In: CVPR (2021)
14. Chen, Z., Fu, Y., Wang, Y.X., Ma, L., Liu, W., Hebert, M.: Image deformation meta-networks for one-shot learning. In: CVPR (2019)
15. Cubuk, E.D., Zoph, B., Mane, D., Vasudevan, V., Le, Q.V.: Autoaugment: Learning augmentation policies from data (2019)
16. Cubuk, E.D., Zoph, B., Shlens, J., Le, Q.V.: Randaugment: Practical automated data augmentation with a reduced search space (2019)
17. Cubuk, E.D., Zoph, B., Shlens, J., Le, Q.: Randaugment: Practical automated data augmentation with a reduced search space. In: Larochelle, H., Ranzato, M., Hadsell, R., Balcan, M., Lin, H. (eds.) *Advances in Neural Information Processing Systems*. vol. 33, pp. 18613–18624. Curran Associates, Inc. (2020), <https://proceedings.neurips.cc/paper/2020/file/d85b63ef0ccb114d0a3bb7b7d808028f-Paper.pdf>
18. Cui, J., Zhong, Z., Liu, S., Yu, B., Jia, J.: Parametric contrastive learning. In: ICCV. pp. 715–724 (2021)
19. Cui, Y., Jia, M., Lin, T.Y., Song, Y., Belongie, S.: Class-balanced loss based on effective number of samples. In: CVPR. pp. 9268–9277 (2019)
20. Deng, J., Dong, W., Socher, R., Li, L.J., Li, K., Fei-Fei, L.: Imagenet: A large-scale hierarchical image database. In: 2009 IEEE conference on computer vision and pattern recognition. pp. 248–255. Ieee (2009)
21. Ding, M., An, B., Xu, Y., Satheesh, A., Huang, F.: SAFLEX: Self-adaptive augmentation via feature label extrapolation. In: *The Twelfth International Conference on Learning Representations* (2024), <https://openreview.net/forum?id=qL6brrBDk2>
22. Dosovitskiy, A., Beyer, L., Kolesnikov, A., Weissenborn, D., Zhai, X., Unterthiner, T., Dehghani, M., Minderer, M., Heigold, G., Gelly, S., Uszkoreit, J., Houshy, N.: An image is worth 16x16 words: Transformers for image recognition at scale. In: ICLR (2021)
23. Dunlap, L., Mohri, C., Zhang, H., Guillory, D., Darrell, T., Gonzalez, J.E., Rohrbach, A., Raghunathan, A.: Using language to extend to unseen domains. *International Conference on Learning Representations (ICLR)* (2023)
24. Dunlap, L., Umino, A., Zhang, H., Yang, J., Gonzalez, J.E., Darrell, T.: Diversify your vision datasets with automatic diffusion-based augmentation (2023)
25. Dvornik, N., Mairal, J., Schmid, C.: Diversity with cooperation: Ensemble methods for few-shot classification. In: ICCV (2019)
26. Feng, C.M., Yu, K., Liu, Y., Khan, S., Zuo, W.: Diverse data augmentation with diffusions for effective test-time prompt tuning (2023)
27. Finn, C., Abbeel, P., Levine, S.: Model-agnostic meta-learning for fast adaptation of deep networks. In: ICML (2017)



28. Frid-Adar, M., Diamant, I., Klang, E., Amitai, M., Goldberger, J., Greenspan, H.: Gan-based synthetic medical image augmentation for increased cnn performance in liver lesion classification. *Neurocomputing* (2018)
29. Geirhos, R., Jacobsen, J.H., Michaelis, C., Zemel, R., Brendel, W., Bethge, M., Wichmann, F.A.: Shortcut learning in deep neural networks. *Nature Machine Intelligence* **2**(11), 665–673 (2020)
30. He, K., Chen, X., Xie, S., Li, Y., Dollár, P., Girshick, R.B.: Masked autoencoders are scalable vision learners. In: *CVPR*. pp. 15979–15988. IEEE (2022)
31. He, K., Chen, X., Xie, S., Li, Y., Dollár, P., Girshick, R.: Masked autoencoders are scalable vision learners (2021)
32. He, K., Fan, H., Wu, Y., Xie, S., Girshick, R.: Momentum contrast for unsupervised visual representation learning. In: *CVPR*. pp. 9729–9738 (2020)
33. He, R., Sun, S., Yu, X., Xue, C., Zhang, W., Torr, P., Bai, S., Qi, X.: Is synthetic data from generative models ready for image recognition? *arXiv preprint arXiv:2210.07574* (2022)
34. Hemmat, R.A., Pezeshki, M., Bordes, F., Drozdal, M., Romero-Soriano, A.: Feedback-guided data synthesis for imbalanced classification (2023)
35. Hendrycks, D., Mu, N., Cubuk, E.D., Zoph, B., Gilmer, J., Lakshminarayanan, B.: AugMix: A simple data processing method to improve robustness and uncertainty. *Proceedings of the International Conference on Learning Representations (ICLR)* (2020)
36. Hong, Y., Zhang, J., Sun, Z., Yan, K.: Safa: Sample-adaptive feature augmentation for long-tailed image classification. In: *ECCV* (2022)
37. Hsu, K., Levine, S., Finn, C.: Unsupervised learning via meta-learning. In: *ICLR* (2018)
38. Huang, S.W., Lin, C.T., Chen, S.P., an Po-Hao Hsu, Y.Y.W., Lai, S.H.: Auggan: Cross domain adaptation with gan-based data augmentation. *European Conference on Computer Vision* (2018)
39. Jain, S., Lawrence, H., Moitra, A., Madry, A.: Distilling model failures as directions in latent space. In: *ArXiv preprint arXiv:2206.14754* (2022)
40. Jang, H., Lee, H., Shin, J.: Unsupervised meta-learning via few-shot pseudo-supervised contrastive learning. In: *The Eleventh International Conference on Learning Representations* (2022)
41. Kang, B., Xie, S., Rohrbach, M., Yan, Z., Gordo, A., Feng, J., Kalantidis, Y.: Decoupling representation and classifier for long-tailed recognition. In: *ICLR* (2020)
42. Khodadadeh, S., Boloni, L., Shah, M.: Unsupervised meta-learning for few-shot image classification. In: *NeurIPS* (2019)
43. Kim, J.H., Choo, W., Song, H.O.: Puzzle mix: Exploiting saliency and local statistics for optimal mixup. In: *International Conference on Machine Learning*. pp. 5275–5285. PMLR (2020)
44. Koohpayegani, S.A., Tejankar, A., Pirsiavash, H.: Mean shift for self-supervised learning (2021)
45. Krause, J., Stark, M., Deng, J., Fei-Fei, L.: 3D object representations for fine-grained categorization. In: *Workshop on 3D Representation and Recognition*. Sydney, Australia (2013)
46. Li, A.C., Prabhudesai, M., Duggal, S., Brown, E., Pathak, D.: Your diffusion model is secretly a zero-shot classifier (2023)
47. Li, B., Han, Z., Li, H., Fu, H., Zhang, C.: Trustworthy long-tailed classification. In: *CVPR*. pp. 6970–6979 (2022)
48. Li, D., Ling, H., Kim, S.W., Kreis, K., Barriuso, A., Fidler, S., Torralba, A.: Bigdatasetgan: Synthesizing imagenet with pixel-wise annotations (2022)

49. Li, J., Tan, Z., Wan, J., Lei, Z., Guo, G.: Nested collaborative learning for long-tailed visual recognition. In: CVPR. pp. 6949–6958 (2022)
50. Li, K., Zhang, Y., Li, K., Fu, Y.: Adversarial feature hallucination networks for few-shot learning. In: CVPR (2020)
51. Li, M., Cheung, Y.m., Lu, Y., et al.: Long-tailed visual recognition via gaussian clouded logit adjustment. In: CVPR. pp. 6929–6938 (2022)
52. Li, T., Cao, P., Yuan, Y., Fan, L., Yang, Y., Feris, R.S., Indyk, P., Katabi, D.: Targeted supervised contrastive learning for long-tailed recognition. In: CVPR. pp. 6918–6928 (2022)
53. Liu, B., Cao, Y., Lin, Y., Li, Q., Zhang, Z., Long, M., Hu, H.: Negative margin matters: Understanding margin in few-shot classification. In: ECCV (2020)
54. Liu, X., Zhang, X., Ma, J., Peng, J., et al.: InstafLOW: One step is enough for high-quality diffusion-based text-to-image generation. In: The Twelfth International Conference on Learning Representations (2023)
55. Liu, Z., Li, S., Wu, D., Liu, Z., Chen, Z., Wu, L., Li, S.Z.: Automix: Unveiling the power of mixup for stronger classifiers. In: Computer Vision–ECCV 2022: 17th European Conference, Tel Aviv, Israel, October 23–27, 2022, Proceedings, Part XXIV. pp. 441–458. Springer (2022)
56. Liu, Z., Miao, Z., Zhan, X., Wang, J., Gong, B., Yu, S.X.: Large-scale long-tailed recognition in an open world. In: CVPR (2019)
57. Lu, Y., Wen, L., Liu, J., Liu, Y., Tian, X.: Self-supervision can be a good few-shot learner. In: European Conference on Computer Vision. pp. 740–758. Springer (2022)
58. Luo, X.J., Wang, S., Wu, Z., Sakaridis, C., Cheng, Y., Fan, D.P., Gool, L.V.: Camdiff: Camouflage image augmentation via diffusion model (2023)
59. Luzi, L., Siahkoohi, A., Mayer, P.M., Casco-Rodriguez, J., Baraniuk, R.: Boomerang: Local sampling on image manifolds using diffusion models (2022)
60. Maji, S., Rahtu, E., Kannala, J., Blaschko, M.B., Vedaldi, A.: Fine-grained visual classification of aircraft. arXiv preprint arXiv:1306.5151 (2013)
61. Mao, J., Xiao, T., Jiang, Y., Cao, Z.: What can help pedestrian detection? (2017)
62. Medina, C., Devos, A., Grossglauser, M.: Self-supervised prototypical transfer learning for few-shot classification. In: ICMLW (2020)
63. Meng, C., He, Y., Song, Y., Song, J., Wu, J., Zhu, J.Y., Ermon, S.: Sdedit: Guided image synthesis and editing with stochastic differential equations. arXiv preprint arXiv:2108.01073 (2021)
64. Meng, C., Rombach, R., Gao, R., Kingma, D., Ermon, S., Ho, J., Salimans, T.: On distillation of guided diffusion models. In: Proceedings of the IEEE/CVF Conference on Computer Vision and Pattern Recognition. pp. 14297–14306 (2023)
65. Menon, A.K., Jayasumana, S., Rawat, A.S., Jain, H., Veit, A., Kumar, S.: Long-tail learning via logit adjustment. In: ICLR (2021)
66. Oquab, M., Darcet, T., Moutakanni, T., Vo, H., Szafraniec, M., Khalidov, V., Fernandez, P., Haziza, D., Massa, F., El-Nouby, A., Assran, M., Ballas, N., Galuba, W., Howes, R., Huang, P.Y., Li, S.W., Misra, I., Rabbat, M., Sharma, V., Synnaeve, G., Xu, H., Jegou, H., Mairal, J., Labatut, P., Joulin, A., Bojanowski, P.: DINOv2: Learning robust visual features without supervision (2023)
67. Peebles, W., Zhu, J.Y., Zhang, R., Torralba, A., Efros, A., Shechtman, E.: GAN-supervised dense visual alignment. In: CVPR (2022)
68. Petryk, S., Dunlap, L., Nasser, K., Gonzalez, J., Darrell, T., Rohrbach, A.: On guiding visual attention with language specification. In: Conference on Computer Vision and Pattern Recognition (CVPR) (2022). <https://doi.org/10.48550/ARXIV.2202.08926>, <https://arxiv.org/abs/2202.08926>

69. Prabhu, V., Yenamandra, S., Chattopadhyay, P., Hoffman, J.: Lance: Stress-testing visual models by generating language-guided counterfactual images. *Advances in Neural Information Processing Systems* **36** (2024)
70. Qiao, S., Liu, C., Shen, W., Yuille, A.: Few-shot image recognition by predicting parameters from activations. In: *CVPR* (2018)
71. Qin, T., Li, W., Shi, Y., Yang, G.: Unsupervised few-shot learning via distribution shift-based augmentation. *arXiv:2004.05805* (2020)
72. Radford, A., Kim, J.W., Hallacy, C., Ramesh, A., Goh, G., Agarwal, S., Sasstry, G., Askell, A., Mishkin, P., Clark, J., Krueger, G., Sutskever, I.: Learning transferable visual models from natural language supervision. In: *ICML* (2021)
73. Ramesh, A., Dhariwal, P., Nichol, A., Chu, C., Chen, M.: Hierarchical text-conditional image generation with clip latents. *arXiv preprint arXiv:2204.06125* **1**(2), 3 (2022)
74. Ramesh, A., Pavlov, M., Goh, G., Gray, S., Voss, C., Radford, A., Chen, M., Sutskever, I.: Zero-shot text-to-image generation. In: *ICML* (2021)
75. Ravi, S., Larochelle, H.: Optimization as a model for few-shot learning. In: *ICLR* (2017)
76. Ren, M., Ravi, S., Triantafyllou, E., Snell, J., Swersky, K., Tenenbaum, J.B., Larochelle, H., Zemel, R.S.: Meta-learning for semi-supervised few-shot classification. In: *International Conference on Learning Representations* (2018), <https://openreview.net/forum?id=HJcSzz-CZ>
77. Rombach, R., Blattmann, A., Lorenz, D., Esser, P., Ommer, B.: High-resolution image synthesis with latent diffusion models. In: *Proceedings of the IEEE/CVF Conference on Computer Vision and Pattern Recognition (CVPR)*. pp. 10684–10695 (June 2022)
78. Rombach, R., Blattmann, A., Lorenz, D., Esser, P., Ommer, B.: High-resolution image synthesis with latent diffusion models. In: *CVPR* (2022)
79. Saharia, C., Chan, W., Saxena, S., Li, L., Whang, J., Denton, E.L., Ghasemipour, K., Gontijo Lopes, R., Karagol Ayan, B., Salimans, T., et al.: Photorealistic text-to-image diffusion models with deep language understanding. *Advances in Neural Information Processing Systems* **35**, 36479–36494 (2022)
80. Sankaranarayanan, S., Balaji, Y., Castillo, C.D., Chellappa, R.: Generate to adapt: Aligning domains using generative adversarial networks. *Conference on Computer Vision and Pattern Recognition (CVPR)* (2018)
81. Sauer, A., Lorenz, D., Blattmann, A., Rombach, R.: Adversarial diffusion distillation. *arXiv preprint arXiv:2311.17042* (2023)
82. Schwartz, E., Karlinsky, L., Shtok, J., Harary, S., Marder, M., Kumar, A., Feris, R.S., Giryes, R., Bronstein, A.M.: Delta-encoder: an effective sample synthesis method for few-shot object recognition. In: *NeurIPS* (2018)
83. Sharmanska, V., Hendricks, L.A., Darrell, T., Quadrianto, N.: Contrastive examples for addressing the tyranny of the majority. *CoRR* **abs/2004.06524** (2020), <https://arxiv.org/abs/2004.06524>
84. Shipard, J., Wiliem, A., Thanh, K.N., Xiang, W., Fookes, C.: Boosting zero-shot classification with synthetic data diversity via stable diffusion. *arXiv preprint arXiv:2302.03298* (2023)
85. Shirekar, O.K., Singh, A., Jamali-Rad, H.: Self-attention message passing for contrastive few-shot learning. In: *Proceedings of the IEEE/CVF Winter Conference on Applications of Computer Vision (WACV)*. pp. 5426–5436 (January 2023)
86. Shorten, C., Khoshgoftaar, T.M.: A survey on image data augmentation for deep learning. *Journal of big data* **6**(1), 1–48 (2019)

87. Singh, A.R., Jamali-Rad, H.: Transductive decoupled variational inference for few-shot classification. *Transactions on Machine Learning Research* (2023), <https://openreview.net/forum?id=bomdTc9HyL>
88. Snell, J., Swersky, K., Zemel, R.S.: Prototypical networks for few-shot learning. In: *NeurIPS* (2017)
89. Su, J.C., Maji, S., Hariharan, B.: When does self-supervision improve few-shot learning? In: *ECCV* (2020)
90. Sung, F., Yang, Y., Zhang, L., Xiang, T., Torr, P.H., Hospedales, T.M.: Learning to compare: Relation network for few-shot learning. In: *CVPR* (2018)
91. Tang, K., Huang, J., Zhang, H.: Long-tailed classification by keeping the good and removing the bad momentum causal effect. *NeurIPS* **33**, 1513–1524 (2020)
92. Touvron, H., Cord, M., Douze, M., Massa, F., Sablayrolles, A., Jégou, H.: Training data-efficient image transformers and distillation through attention (2021)
93. Touvron, H., Cord, M., Jégou, H.: Deit iii: Revenge of the vit. In: *ECCV* (2022)
94. Trabucco, B., Doherty, K., Gurinas, M., Salakhutdinov, R.: Effective data augmentation with diffusion models (2023)
95. Tritrong, N., Rewatbowornwong, P., Suwajanakorn, S.: Repurposing gans for one-shot semantic part segmentation. In: *IEEE Conference on Computer Vision and Pattern Recognition (CVPR)* (2021)
96. Vinyals, O., Blundell, C., Lillicrap, T., Wierstra, D., et al.: Matching networks for one shot learning. In: *NeurIPS* (2016)
97. Wah, C., Branson, S., Welinder, P., Perona, P., Belongie, S.: The caltech-ucsd birds-200-2011 dataset (2011)
98. Wang, H., Deng, Z.H.: Contrastive prototypical network with wasserstein confidence penalty. In: *European Conference on Computer Vision*. pp. 665–682. Springer (2022)
99. Wang, H., Fu, S., He, X., Fang, H., Liu, Z., Hu, H.: Towards calibrated hypersphere representation via distribution overlap coefficient for long-tailed learning. In: *ECCV* (2022)
100. Wang, X., Lian, L., Miao, Z., Liu, Z., Yu, S.X.: Long-tailed recognition by routing diverse distribution-aware experts. In: *ICLR*. OpenReview.net (2021)
101. Wu, Z., Efros1, A.A., Yu, S.X.: Improving generalization via scalable neighborhood component analysis. In: *ECCV* (2018)
102. Xu, Y., Li, Y.L., Li, J., Lu, C.: Constructing balance from imbalance for long-tailed image recognition. In: *ECCV*. pp. 38–56. Springer (2022)
103. Xu, Z., Liu, R., Yang, S., Chai, Z., Yuan, C.: Learning imbalanced data with vision transformers (2023)
104. Xuan, H., Stylianou, A., Liu, X., Pless, R.: Hard negative examples are hard, but useful (2021)
105. Ye, H.J., Hu, H., Zhan, D.C., Sha, F.: Few-shot learning via embedding adaptation with set-to-set functions. In: *IEEE/CVF Conference on Computer Vision and Pattern Recognition (CVPR)*. pp. 8808–8817 (2020)
106. Ye, H.J., Hu, H., Zhan, D.C., Sha, F.: Few-shot learning via embedding adaptation with set-to-set functions. In: *CVPR* (2020)
107. Yun, S., Han, D., Oh, S.J., Chun, S., Choe, J., Yoo, Y.: Cutmix: Regularization strategy to train strong classifiers with localizable features. In: *ICCV*. pp. 6023–6032 (2019)
108. Zhang, H., Cisse, M., Dauphin, Y.N., Lopez-Paz, D.: mixup: Beyond empirical risk minimization. In: *ICLR* (2018)
109. Zhang, S., Li, Z., Yan, S., He, X., Sun, J.: Distribution alignment: A unified framework for long-tail visual recognition. In: *CVPR*. pp. 2361–2370 (2021)

110. Zhang, Y., Hooi, B., Hong, L., Feng, J.: Test-agnostic long-tailed recognition by test-time aggregating diverse experts with self-supervision. arXiv preprint arXiv:2107.09249 (2021)
111. Zhang, Y., Ling, H., Gao, J., Yin, K., Lafleche, J.F., Barriuso, A., Torralba, A., Fidler, S.: Datasetgan: Efficient labeled data factory with minimal human effort. In: CVPR (2021)
112. Zhong, Z., Cui, J., Liu, S., Jia, J.: Improving calibration for long-tailed recognition. In: CVPR. pp. 16489–16498. Computer Vision Foundation / IEEE (2021)
113. Zhou, Z., Qiu, X., Xie, J., Wu, J., Zhang, C.: Binocular mutual learning for improving few-shot classification. In: ICCV (2021)
114. Zhu, J., Wang, Z., Chen, J., Chen, Y.P.P., Jiang, Y.G.: Balanced contrastive learning for long-tailed visual recognition. In: CVPR. pp. 6908–6917 (2022)

## A Appendix

### A.1 Comparison with Long-Tail methods

We present a comprehensive version of Table 3 to benchmark the performance with different backbone architectures (e.g., ResNet50) and to compare against previous long-tail baselines; this is detailed in Table A1.

### A.2 Details of Fine-grained Dataset

We provide detailed information around fine-grained datasets in Table A2, as discussed in Section 3.3.

**Table A1: Long-Tailed ImageNet-LT:** We compare different augmentation methods on ImageNet-LT and report Top-1 accuracy for “Few”, “Medium”, and “Many” sets. † indicates results with ResNeXt50. \*: indicates training with 384 resolution so is not directly comparable with other methods with 224 resolution. On the “Few” set and LiVT method, our augmentations improve the accuracy by 11.7 points compared to LiVT original augmentation and 4.4 points compared to Txt2Img.

ResNet-50				
Method	Many	Med.	Few	Overall Acc
CE [19]	64.0	33.8	5.8	41.6
LDAM [8]	60.4	46.9	30.7	49.8
c-RT [41]	61.8	46.2	27.3	49.6
$\tau$ -Norm [41]	59.1	46.9	30.7	49.4
Causal [91]	62.7	48.8	31.6	51.8
Logit Adj. [65]	61.1	47.5	27.6	50.1
RIDE(4E)† [100]	68.3	53.5	35.9	56.8
MiSLAS [112]	62.9	50.7	34.3	52.7
DisAlign [109]	61.3	52.2	31.4	52.9
ACE† [7]	71.7	54.6	23.5	56.6
PaCo† [18]	68.0	56.4	37.2	58.2
TADe† [110]	66.5	<b>57.0</b>	43.5	58.8
TSC [52]	63.5	49.7	30.4	52.4
GCL [51]	63.0	52.7	37.1	54.5
TLC [47]	68.9	55.7	40.8	55.1
BCL† [114]	67.6	54.6	36.6	57.2
NCL [49]	67.3	55.4	39.0	57.7
SAFA [36]	63.8	49.9	33.4	53.1
DOC [99]	65.1	52.8	34.2	55.0
DLSA [102]	67.8	54.5	38.8	57.5
ViT-B				
LiVT* [103]	76.4	59.7	42.7	63.8
ViT [22]	50.5	23.5	6.9	31.6
MAE [30]	74.7	48.2	19.4	54.5
DeiT [93]	70.4	40.9	12.8	48.4
LiVT [103]	73.6	56.4	41.0	60.9
LiVT + Img2Img <sup>L</sup>	74.3	56.4	34.3	60.5
LiVT + Img2Img <sup>H</sup>	73.8	56.4	45.3	61.6
LiVT + Txt2Img	<b>74.9</b>	55.6	48.3	62.2
LiVT + GeNIe (r=0.8)	74.5	56.7	50.9	62.8
LiVT + GeNIe-Ada	74.0	<b>56.9</b>	<b>52.7</b>	<b>63.1</b>

**Table A2:** Train and test split details of the fine-grained datasets. We use the provided train set for few-shot task generation, and the provided test sets for our evaluation. For the Aircraft dataset we use manufacturer hierarchy.

Dataset	Classes	Train samples	Test samples
CUB200 [97]	200	5994	5794
Food101 [6]	101	75750	25250
Cars [45]	196	8144	8041
Aircraft [60]	41	6,667	3333

### A.3 More Visualizations

Additional qualitative results resembling the style presented in Figure 4 are presented in Figure A1, and more visuals akin to Figure 2 can be found in Figure A2. Moreover, we also present more visualization similar to the style in Figure 5 in Figure A3.



**Fig. A1: Visualization of Generative Samples:** More visualization akin to Figure 4. We compare GeNIe with two baselines: **Img2Img<sup>L</sup> augmentation** uses both image and text prompt from the same category, resulting in less challenging examples. **Txt2Img augmentation** generates images based solely on a text prompt, potentially deviating from the task’s visual domain. **GeNIe augmentation** incorporates the target category name in the text prompt along with the source image, producing desired images with an optimal amount of noise, balancing the impact of the source image and text prompt.

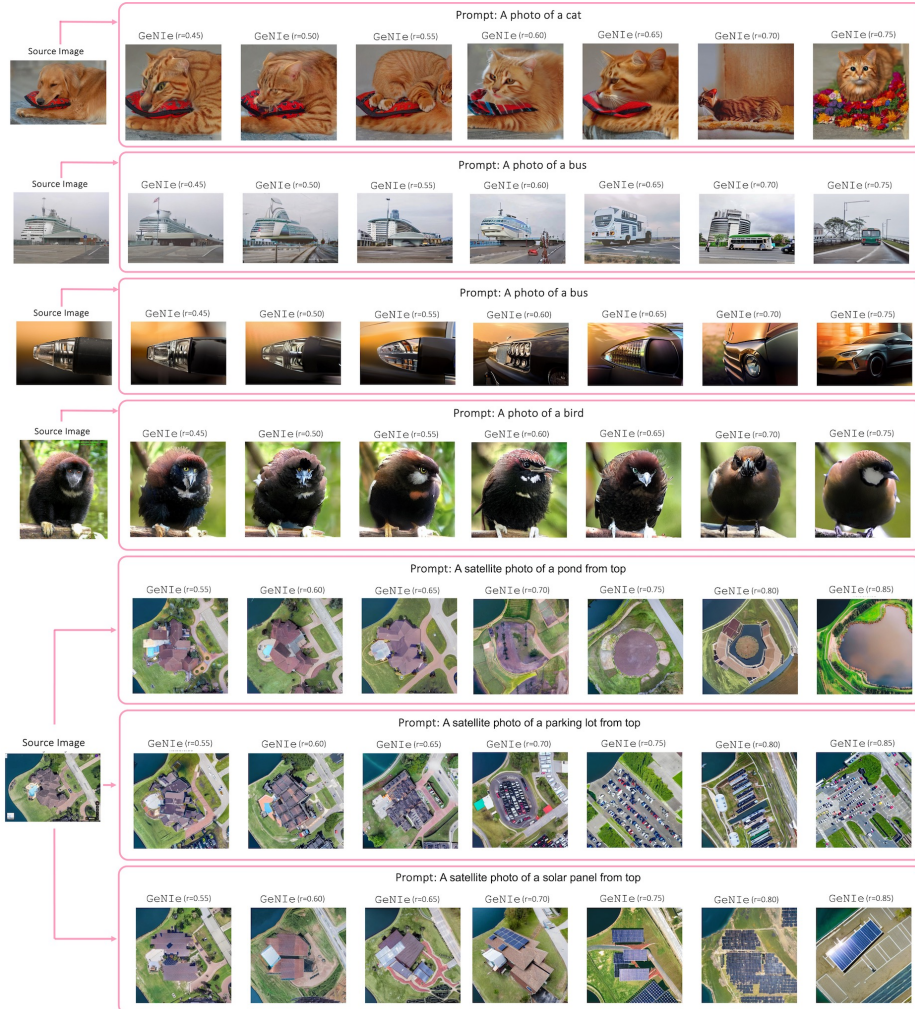


**Fig. A2: Effect of noise in GeNIe:** Akin to Figure 2, we use GeNIe to create augmentations with varying noise levels. As is illustrated in the examples above, a reduced amount of noise leads to images closely mirroring the semantics of the source images, causing a misalignment with the intended target label.



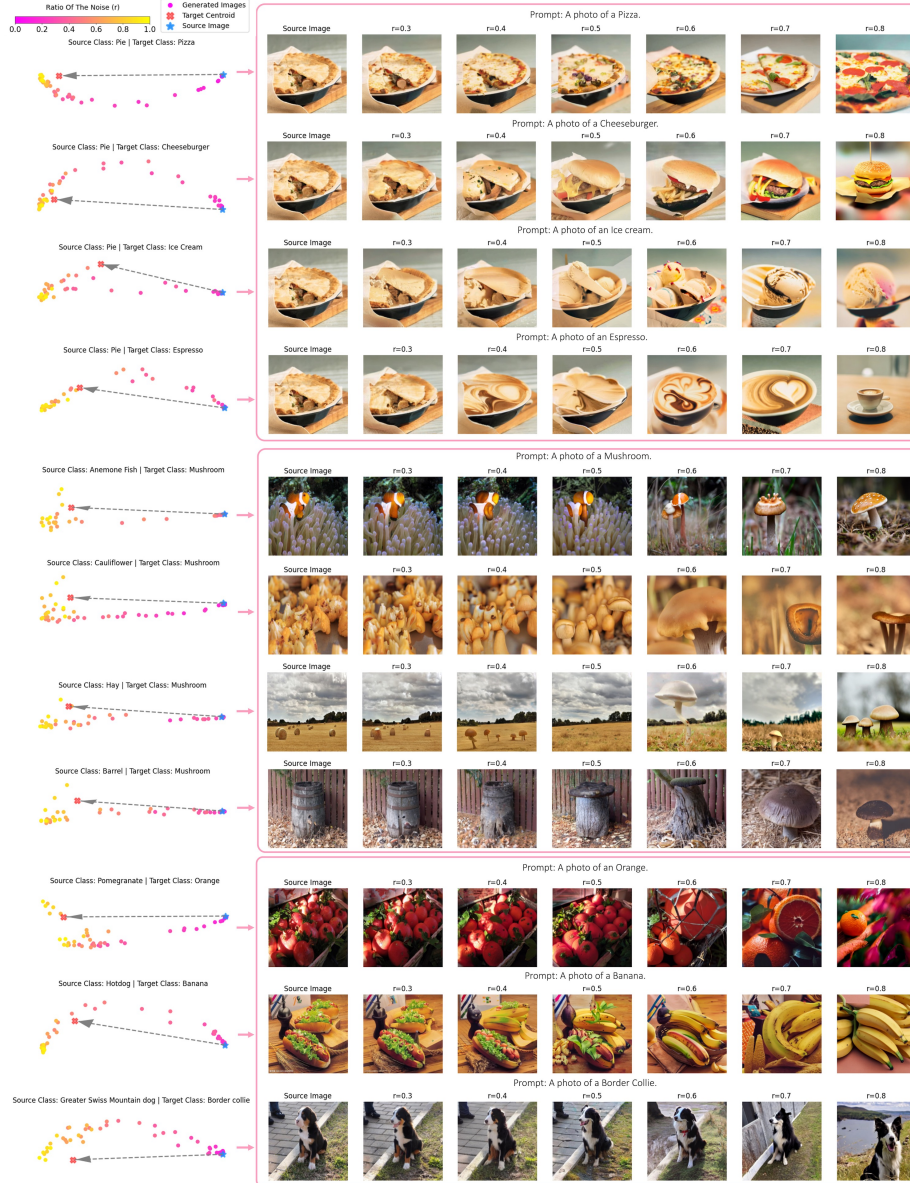


**Fig. A3: Effect of noise in GeNIe:** Similar to Figure 5, we pass all the generated augmentations through the DinoV2 ViT-G model, which acts as our oracle model, to obtain their associated embeddings. Subsequently, we employ PCA for visualization purposes. The visualization reveals that the magnitude of semantic transformations is contingent upon both the source image and the specified target category.